

## Role of hydrogen on the ZnO(000 $\bar{1}$ )-(1×1) surface

S. E. Chamberlin,<sup>1</sup> C. J. Hirschmugl,<sup>1,\*</sup> S. T. King,<sup>2</sup> H. C. Poon,<sup>1</sup> and D. K. Saldin<sup>1</sup>

<sup>1</sup>*Department of Physics and Laboratory for Surface Studies, University of Wisconsin - Milwaukee, Milwaukee, Wisconsin 53211, USA*

<sup>2</sup>*Department of Physics, University of Wisconsin - La Crosse, La Crosse, Wisconsin 54601, USA*

(Received 8 July 2010; revised manuscript received 17 May 2011; published 8 August 2011)

A structural study has been performed on the polar ZnO(000 $\bar{1}$ )-(1×1) surface using *ab initio* calculations and low-energy electron diffraction (LEED). The experiment was performed with a delay line detector LEED system to minimize electron damage of the surface. The top O-Zn interlayer spacing was found to be  $0.51 \pm 0.04$  Å, a  $16\% \pm 6\%$  contraction from the bulk spacing. The second and third interlayer spacings were found to be more bulklike at  $2.01 \pm 0.02$  Å ( $0 \pm 1\%$ ) and  $0.61 \pm 0.02$  Å ( $0 \pm 3\%$ ), respectively. When compared with calculations of several hydrogen coverages, the experimental surface relaxations suggest a 1/3 monolayer (ML) coverage of hydrogen. The density of states of the 1/3 ML H-terminated surface indicates that the O-2*p* level is raised above the Fermi energy with respect to its bulk energy. However, the O-2*p* level is shifted to lower energy when compared with the clean, H-free surface.

DOI: 10.1103/PhysRevB.84.075437

PACS number(s): 68.47.Gh, 61.05.jh, 71.15.Mb, 73.20.At

### I. INTRODUCTION

Zinc oxide is a widely studied wide-band-gap semiconductor with a variety of technologically important applications.<sup>1,2</sup> As shown by the side view in Fig. 1, the wurtzite crystalline structure of ZnO forms alternating planes of zinc and oxygen atoms when cut perpendicular to the *c* axis. A result of such stacking is a net dipole moment perpendicular to the surface. The dipole moment, and corresponding surface energy, have been shown to diverge with increasing sample size,<sup>3</sup> thus leading to the so-called “polar instability problem.” In order to suppress the dipole moment and thus stabilize the surface, some form of charge compensation must occur at the surface.<sup>3</sup>

For polar ZnO surfaces, this means that the O face becomes less negatively charged and the Zn face becomes less positively charged. To achieve this, several mechanisms are possible<sup>4</sup> including (1) charge transfer from the O to Zn surface, which may result in “metallization;” (2) vacancies at the surface—these may take the form of an ordered reconstruction or remain disordered; (3) adsorption of charged species, e.g., a hydroxylated surface with H<sup>+</sup>. Additionally, a combination of these ideal mechanisms is also possible. For many polar oxide materials, stabilization is often achieved by surface reconstruction. However, clean, polar ZnO surfaces are often observed to remain unreconstructed. This observation may require considering the other compensation mechanisms in order to understand the stability of polar ZnO surfaces.

On the Zn-polar (1×1) surface, scanning tunneling microscopy (STM) has shown terraces with a triangular shape and a step height of one ZnO double layer.<sup>5</sup> A high density of triangular pits and islands are consistently observed on these terraces. The step edges are O terminated, which changes the stoichiometry of the surface. An analysis of the islands and pits reveals that  $\sim 1/4$  of the Zn ions are missing, which fulfills method (2) as a means of stabilizing the surface.<sup>6</sup>

However, this characteristic island and pit structure was not observed for the O-polar [denoted ZnO(000 $\bar{1}$ )] (1×1) surface.<sup>5</sup> No evidence for significant oxygen vacancies has been found,<sup>7,8</sup> suggesting a stoichiometric surface that is not stabilized by vacancies. An early surface x-ray diffraction (SXRD) and density-functional theory (DFT) study by Wander

*et al.* suggested that a clean, unreconstructed surface could be stable with incomplete charge transfer between the Zn- and O-polar surfaces, resulting in metallic surface states.<sup>9</sup> However, several recent studies of newly found reconstructions have called into question this stabilization mechanism for the unreconstructed (1×1) surface. Among them, He-atom scattering of hydrogen-free ZnO(000 $\bar{1}$ ) has observed a (1×3) reconstruction of the surface, which deconstructs to a (1×1) upon H exposure, suggesting that H plays a role in stabilizing the (1×1) surface.<sup>10</sup> Even more recently, a previously unreported ( $\sqrt{3} \times \sqrt{3}$ )R30° reconstruction was found, the formation of which appears to be suppressed in the presence of hydrogen.<sup>11</sup> Additionally, a recent DFT study suggests that up to 1/2 monolayer (ML) of hydrogen coverage may be energetically favorable on O-polar ZnO surfaces.<sup>12</sup>

In this paper we present a low-energy electron diffraction (LEED)-IV study of the O-polar ZnO(000 $\bar{1}$ )-(1×1) surface using a femto-ampere LEED instrument constructed to rapidly collect high quality LEED data with low total electron exposures.<sup>13</sup> The electron gun of this instrument is capable of achieving beam currents in the femto-ampere range, making it ideal for studying weakly bound systems and insulators. Although low-energy electrons are not directly sensitive to the presence of hydrogen due to its small scattering cross section, the effect of hydrogen on the oxygen and zinc surface layers should be observable. Therefore, the structural results of the LEED-IV analysis are combined with first-principles DFT calculations to examine the effect of hydrogen adsorption.

### II. EXPERIMENTAL DETAILS

The ZnO(000 $\bar{1}$ ) single-crystal sample was obtained from CrysTec Corporation. The surface was EPI-polished with the surface roughness  $< 5$  Å. The (1×1) surface was prepared in UHV with several cycles of Ne<sup>+</sup> sputtering and subsequent annealing to 650 °C.

The LEED measurements were performed with a low-current, pulse-counting and high-count-rate delay line detector LEED (DL-LEED) system (by OCI Vacuum Microengineering and Reontdek<sup>13</sup>). This system uses a low-current electron gun, microchannel plates for charge amplification, and delay

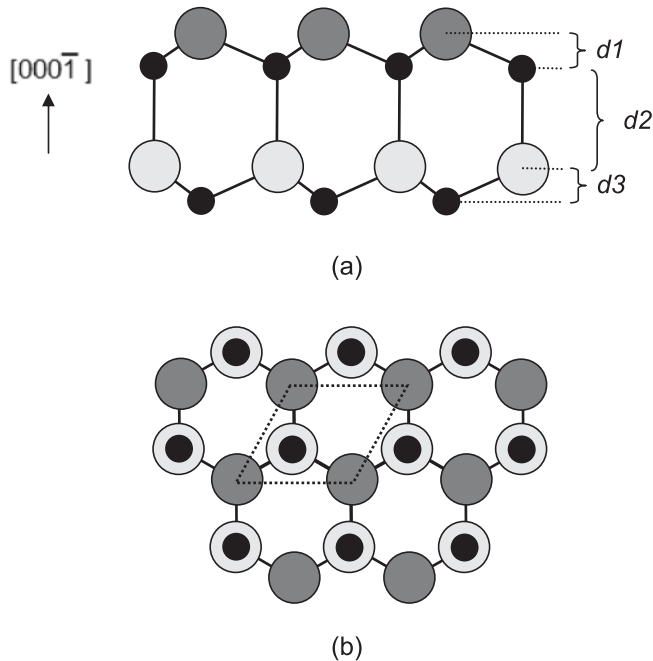


FIG. 1. Side view (a) and top view (b) of the O-polar ZnO(000 $\bar{1}$ ) surface. Oxygen and zinc atoms are represented by large and small circles, respectively. The first three interlayer spacings are defined in (a), and a  $(1 \times 1)$  unit cell is outlined in (b).

line anode planes for signal detection. This allows for the minimization of charging effects and electron-beam-induced damage on insulating surfaces. The details of the DLD-LEED system and comparisons with other systems can be found in Ref. 13, and further discussions of the low-electron dose can be found in Refs. 13 and 14.

Since all stray electrons can be detected by the DLD-LEED, all electron sources (i.e., ion gauge, ion pump) are either turned off or isolated from the UHV chamber. The residual pressure of the UHV chamber, maintained by a Varian V-250 turbo pump, was better than  $1 \times 10^{-9}$  torr. All measurements were taken at 300 K.

### III. THEORETICAL DETAILS

#### A. LEED

The tensor LEED package of Barbieri and Van Hove<sup>15</sup> was used for the LEED intensity calculations. The phase shifts were generated from a self-consistent potential calculated from the FLEUR program.<sup>16</sup> For the energy range of 50–350 eV, the maximum angular momentum quantum number  $l_{\max}$  was taken to be 7. It was found that higher angular momenta have little effect on the IV curves since their phase shifts, for both Zn and O atoms, are very small even at 350 eV. The imaginary part of the inner potential was assumed to vary as the  $1/3$  power of energy with a value of 5.0 eV at 90 eV. The atomic coordinates, the real part of the inner potential, and the thermal-vibration amplitudes of the atoms were adjusted to best fit to the experimental data. For this purpose, the Pendry  $R$  factor ( $R_p$ ) (Ref. 17) was applied as a quantitative measure of the difference between the calculated and experimental spectra.

#### B. DFT

DFT calculations were performed with the projector augmented wave (PAW) method<sup>18,19</sup> in the Vienna ab-initio Simulation Package (VASP).<sup>20–23</sup> The exchange correlation was treated within the generalized gradient approximation (GGA) using the functional of Perdew, Burke, and Ernzerhof (PBE).<sup>24</sup> A dipole correction was applied to eliminate the artificial electrostatic field between periodic supercells. For the clean surface, up to 20 double layers of Zn and O atoms were used in the slab until the structure converged. For the hydrogen-covered surfaces, eight double layers were used. All slabs are asymmetric with the bottom half fixed. Structural optimizations were performed until the residue forces were smaller than 0.01 eV/Å.

### IV. RESULTS

#### A. LEED

At normal incidence, the LEED pattern of ZnO(000 $\bar{1}$ ) has sixfold symmetry due to the existence of two domains rotated by  $60^\circ$  with respect to one another.<sup>25</sup> The domain boundaries are double steps created by the removal of a double layer of Zn-O atoms, which leads to the exposure of the next double layer in the wurtzite structure, rotated with respect to the top double layer. At normal incidence, the number of nonequivalent beams visible to our detector would be insufficient for a structural analysis. Therefore, IV measurements were conducted at  $7^\circ$  off-normal to break the surface symmetry. The incident angles were optimized in the calculation and found to be  $7.2^\circ$  from the surface normal with an azimuth along the  $(1,1)$  and  $(-1,-1)$  direction. Measurements were taken with incident electron energies from 42 to 350 eV in 4-eV steps. From the observed diffraction pattern at each energy, IV curves having a total energy range of approximately 1000 eV were extracted from seven nonequivalent beams.

The LEED calculations were performed with the top six atomic layers allowed to relax from bulk until their positions converged to within 0.002 Å. The  $R$  factor of the optimized structure was found to be  $R_p = 0.15$ , with the best-fit surface and bulk thermal-vibration amplitudes equal to 0.19 and 0.16 Å, respectively. The experimental and the simulated best-fit spectra are compared in Fig. 2. This best-fit structure suggests the first interlayer spacing,  $d1$ , of the ZnO(000 $\bar{1}$ ) surface to be  $0.51 \pm 0.04$  Å, a  $16\% \pm 6\%$  contraction from the bulk spacing. However, the second and third interlayer spacings ( $d2$  and  $d3$ ) are found to be much more bulklike at  $2.01 \pm 0.02$  Å ( $0 \pm 1\%$ ) and  $0.61 \pm 0.02$  Å ( $0 \pm 3\%$ ), respectively.

To test the influence of oxygen defects, we have also repeated our LEED calculations with oxygen vacancies. The Pendry  $R$  factor versus % oxygen vacancies is shown in Fig. 3. Since the standard deviation of the  $R$  factor is about 0.02, it is clear that almost no oxygen vacancies (less than 25%) were present on our sample, and did not play an important role in stabilizing the surface.

#### B. DFT

Since previous experimental works indicate that the  $(1 \times 1)$  surface may be stabilized by hydrogen,<sup>10</sup> DFT calculations have been employed to investigate the adsorption of hydrogen and the effect this may have on our results. (The LEED

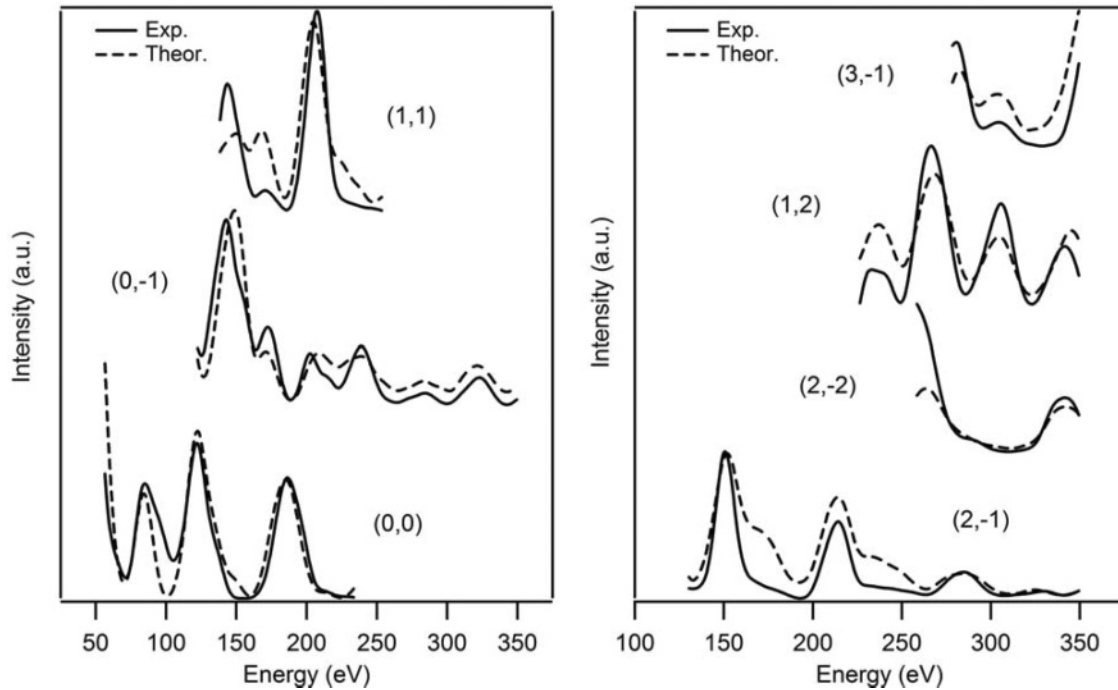


FIG. 2. Comparison of the experimental (solid line) and best-fit calculated (dashed line) spectra of seven nonequivalent beams for the ZnO(000 $\bar{1}$ )-(1 $\times$ 1) surface. The average Pendry  $R$  factor is 0.15.

calculation itself was repeated with up to 1/3 ML of disordered hydrogen on the surface; the effect was found to be negligible.) First the bulk lattice parameters were calculated using the PBE approximation. The results are listed in Table I. These parameters were used in our surface DFT calculations for the bottom half of the slab to simulate the effects of a fixed bulk environment. They were found to agree reasonably well with the results of a previous study.<sup>26</sup>

DFT calculations were repeated for the clean surface, and for 1/3, 1/2, and 1 ML coverages of hydrogen. Although the observed LEED pattern is (1 $\times$ 1), which indicates that any possible fractional hydrogen adsorption is disordered, we have simulated the effect of hydrogen atoms on the surface structure by using the smallest ordered unit cell for the partially

covered surfaces, i.e., a ( $\sqrt{3} \times \sqrt{3}$ ) cell for 1/3 ML and a (1 $\times$ 2) cell for 1/2 ML. Table II lists the resulting average percent change from bulk for the first three interlayer spacings. These calculations suggest that the first interlayer spacing,  $d1$ , is strongly dependent on the hydrogen coverage. For the hydrogen-free surface,  $d1$  is contracted 50% from the bulk, while a fully hydrogen-terminated surface results in a 25% expansion. The layers below  $d1$  are also impacted by the amount of hydrogen on the surface. The second interlayer spacing is initially expanded for a hydrogen-free surface, and becomes contracted with increasing hydrogen coverage. Conversely,  $d3$  is initially contracted and becomes expanded. Neither of these layers exhibits the dramatic dependence seen in  $d1$ .

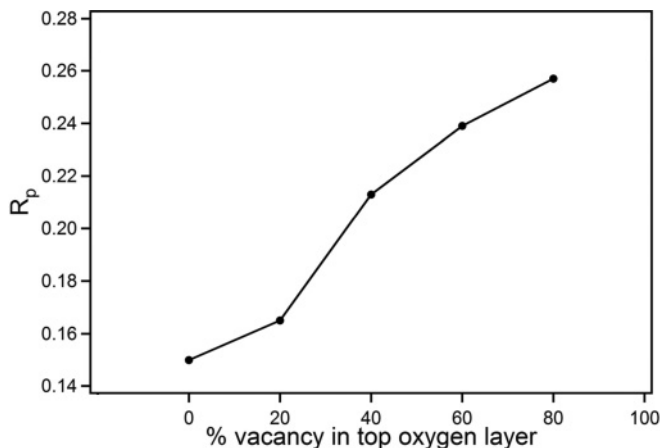


FIG. 3. Pendry  $R$  factor as a function of % oxygen vacancies considered in the top oxygen layer.

## V. DISCUSSION

### A. Literature review

We first compare the interlayer spacings determined from the present LEED-IV analysis with what has been reported in the literature. Our results for the relaxations of the top three layers are compared with previous experimental results in Table III. The values for the top interlayer relaxation vary between 0% to an almost 39% contraction. A previous

TABLE I. Bulk lattice parameters for ZnO.

	VASP	Meyer (Ref. 26)
$a$ (Å)	3.287	3.282
$c$ (Å)	5.318	5.291
$u$	0.3783	0.3792

TABLE II. Average percent change from bulk for the first three interlayer spacings as calculated for 0, 1/3, 1/2, and 1 ML hydrogen-covered surfaces.

Layer	0 ML	1/3 ML	1/2 ML	1 ML
$\% \Delta d1$	-50.09%	-19.30%	-3.56%	+24.6%
$\% \Delta d2$	+5.63%	+1.94%	-0.35%	-3.85%
$\% \Delta d3$	-16.20%	-8.68%	-0.08%	+16.20%

LEED study<sup>27</sup> concluded that there is no top layer relaxation. However, this study by Duke *et al.* included data and analysis of a small energy range from only one beam, which is quite insufficient for a proper structural analysis by modern standards. Moreover, since the (0,0) beam was the only measurement, it is clear that the incident beam direction was a few degrees off-normal, but this was not reported or taken into account in the analysis. Without knowing the exact sample orientation, the LEED analysis with only one domain adds uncertainty to the accuracy of the reported results. The present study, in contrast, has measured and included a significantly larger energy range ( $\sim 1000$  eV) from seven off-normal, nonequivalent beams. The angle of the incident beam was determined experimentally and confirmed and refined during data analysis.

The top interlayer spacing of the LEED-IV analysis also differs from the prominent study by Wander *et al.*, which suggests a much larger contraction of 38.7%.<sup>9</sup> It seems unlikely that the experimental surface in the current study represents a truly clean surface as proposed by Wander *et al.* However, it is unclear whether these authors have considered a two-domain structure, which may explain the discrepancy.

Closer to the present LEED-IV analysis are the results of a grazing incidence x-ray diffraction (GIXD) study, which found the first interlayer spacing of the so-called clean surface to be contracted by almost 20%.<sup>8</sup> Again, as in the Wander *et al.* study, metallization was proposed as the stabilization mechanism, but the differing structural parameters between these two x-ray studies suggests that the mechanism is not completely understood.

### B. DFT spacings

The strong response of the top interlayer spacing to hydrogen adsorption suggests that the amount of inward relaxation found in the LEED-IV analysis could indicate the quantity of hydrogen present on the “clean” ( $1 \times 1$ ) surface. In Fig. 4, the relaxations of the top three interlayers (red lines) are plotted as a function of hydrogen coverage for 0, 1/2, and

TABLE III. The current LEED-IV interlayer spacings compared with the relaxations of the top three layers from previous experimental results.

Layer	LEED (present)	LEED (Ref. 27)	SXRD (Ref. 9)	GIXD (Ref. 8)
$\% \Delta d1$	$-16\% \pm 6\%$	0%	$-38.7\% \pm 9.5\%$	$-19.7\% \pm 4.9\%$
$\% \Delta d2$	$0\% \pm 1\%$		$+1.8\% \pm 2.4\%$	
$\% \Delta d3$	$0\% \pm 3\%$		$-4.9\% \pm 7.7\%$	

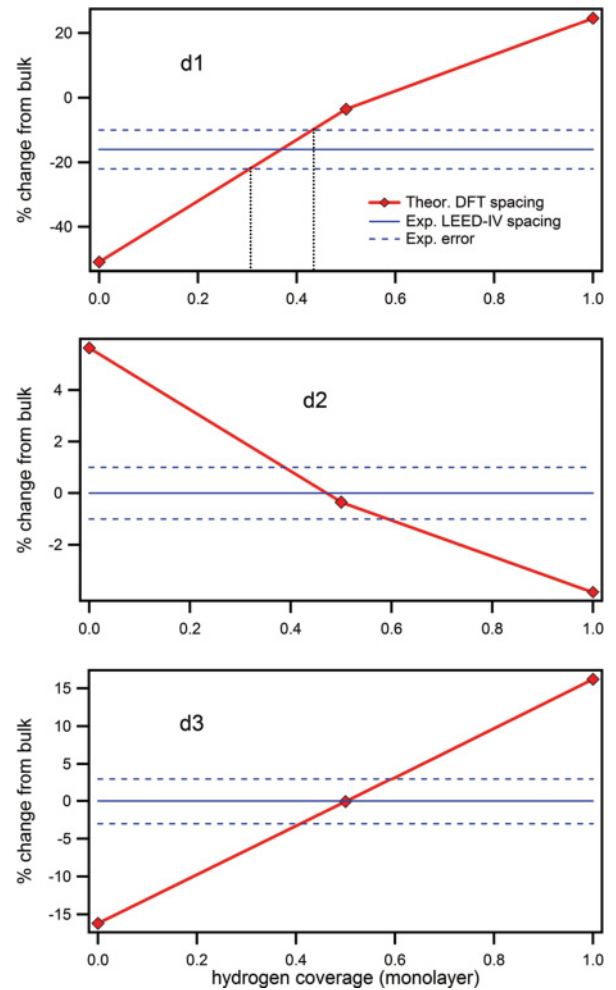


FIG. 4. (Color online) % change from bulk for  $d1$ ,  $d2$ , and  $d3$  as a function of hydrogen coverage. Plotted are both the spacings calculated from DFT in red (thick dark-gray line) and the values derived from the LEED-IV analysis in blue (thin black line).

1 ML as listed in Table II. Also plotted are the values derived from the LEED-IV analysis (blue lines). A hydrogen coverage of about 1/3 to 4/10 of a monolayer is predicted by using the experimental error bars (dashed blue lines) to evaluate  $d1$  in particular. Accordingly, the structural relaxations of a 1/3 ML hydrogen-coverage (see Table II) were compared with the experiment. The ( $\sqrt{3} \times \sqrt{3}$ ) cell used for this calculation has a total of three surface oxygen atoms, one of which is bonded to a hydrogen atom. The first interlayer spacing is found by averaging 2:1 the two different O-Zn spacings in this structure.  $\% \Delta d1 = -33\%$  where the top oxygen atoms are bare, and  $\% \Delta d1 = +9.7\%$  where the top oxygen atom is bonded to hydrogen. The average  $\% \Delta d1$  is thus equal to  $-19.3\%$ , and agrees with the experimental value ( $-16 \pm 6\%$ ). This suggested fractional coverage of hydrogen on the surface provides some of the necessary charge compensation to stabilize the ( $1 \times 1$ ) O-polar surface.

### C. Ordered vs islanding

An obvious question that arises from the drastic influence that adsorbed hydrogen has on the first interlayer spacing is,

“Why are no fractional order spots observed in the LEED pattern?” Since the average value of  $dI$  determined by the DFT calculation for 1/3 ML hydrogen-coverage matches the experimental result, one may think this immediately indicates the existence of an ordered surface layer of hydrogen. Indeed, if hydrogen were adsorbed in a periodic nature, as it is in the DFT calculations, one would expect the appearance of fractional order LEED spots corresponding to the longer length scale of the  $\sqrt{3}$  periodicity. However, since no fractional order spots are observed in the collected data, it is obvious that the hydrogen does not exist in a completely ordered surface layer.

Since LEED measures the average long-range periodicity of a surface rather than the local structure, it is conceivable that the LEED experiment is simultaneously measuring terraces which are both H-saturated as well as H-free. However, arguing against the formation of large hydrogen domains is the energy difference between an ordered surface layer of hydrogen and a “patchy” surface with areas that are H-saturated. For the ordered 1/3 ML hydrogen-covered surface, the energy per unit cell of the slab is  $-73.18$  eV. The energy of the patchy surface is found by a weighted average of the energies of a H-saturated and a H-free surface:  $\frac{1}{3}(-75.47 \text{ eV}) + \frac{2}{3}(-71.38 \text{ eV})$ . This yields an energy per unit cell of  $-72.74$  eV. With a difference of  $\sim 0.4$  eV, the ordered surface is more stable than the patchy surface. This value is consistent with findings by Meyer that, even at low coverage, repulsive forces exist between adsorbed hydrogen atoms.<sup>12</sup> Therefore, it is suggested that the terminating hydrogen may exist as a two-dimensional lattice gas. When time averaged over the duration of the LEED experiment, it would exhibit a  $1 \times 1$  periodicity due to the transient nature of hydrogen adsorption sites. However, the authors cannot exclude the existence of a static, disordered hydrogen overlayer, which may also exhibit a  $1 \times 1$  periodicity.

#### D. Density of states

In addition to the geometric structure of the O-polar ZnO surface, the electronic structure is also of interest. While

several theoretical studies, including that by Wander *et al.*, have predicted the presence of 2D metallic surface states for the (000 $\bar{1}$ ) surface, they have not been experimentally observed. Angle-resolved photoemission experiments indicate that there is no significant charge transfer between surface and subsurface atoms.<sup>28</sup> Additionally, scanning tunneling spectroscopy of the surface shows only a small shift of the filled states toward the Fermi level, but it is not significant enough to be considered metallic.<sup>5</sup>

Comparison between the density of states (DOS) per atom for the top oxygen layer of the clean surface and the 1/3 ML hydrogen-covered surface are shown in Figs. 5(a) and 5(b). The bulk O-2s core level is split in the presence of hydrogen for the surface with 1/3 ML hydrogen. The O-2s of the oxygen atom located directly under the hydrogen atom is chemically shifted away from the Fermi level by 2.6 eV. The O-2s of the oxygen atoms without hydrogen is shifted slightly by 0.9 eV toward the Fermi level. This is almost the same as the surface core-level shift on the clean surface. Similar effects were found on the 1 ML hydrogen-covered and clean surfaces of MgO(111).<sup>29</sup> In this study, the O-derived 2s and 1s states at the surface were found to be shifted toward higher binding energy for the OH-terminated surface. The chemical shift of the O-1s level was also observed by x-ray photoelectron spectroscopy (XPS). Similar experiments have not been done for the ZnO(000 $\bar{1}$ ) surface to the authors’ knowledge. However, the effects are likely to be much smaller.

In previous studies,<sup>9,26</sup> it was shown that for a clean surface, stabilization occurred with charge transferred from the oxygen layer on one side of the slab to the Zn atoms on the other side. This results in the O-2p level being raised above the Fermi energy with respect to its bulk energy level, and the corresponding lowering of the Zn-4s on the other side. On the 1/3 ML hydrogen-covered surface, the O-2p level is split due to the presence of hydrogen, and it is shifted to lower energy compared to the clean surface [see inset in Fig. 5(b)]. The cause of this shift can be seen in Fig. 5(c), which shows the local DOS for an oxygen atom located directly below a hydrogen

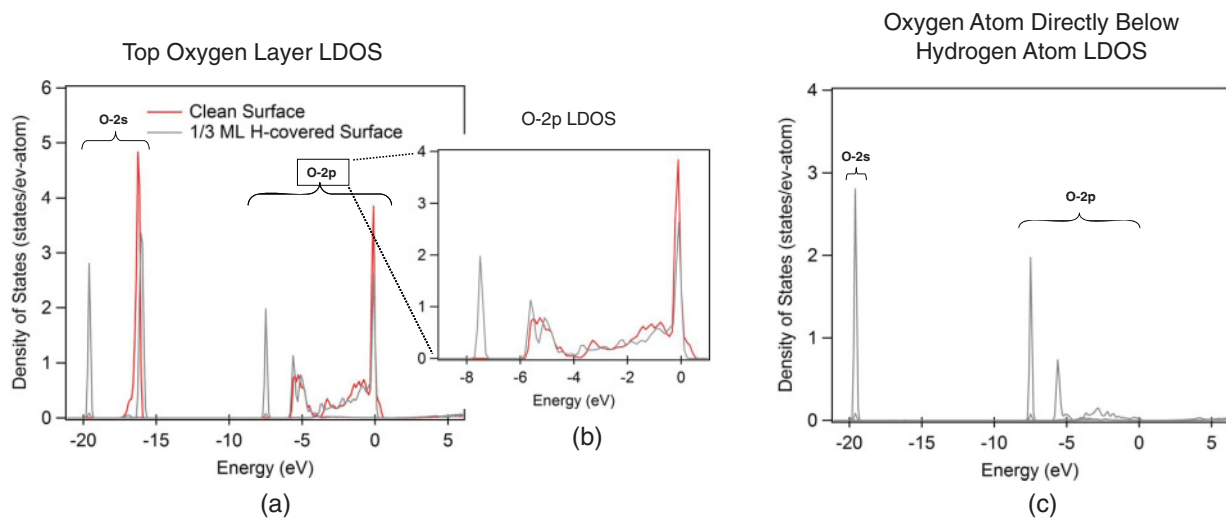


FIG. 5. (Color online) (a) Local DOS per atom of the top oxygen layer. Clean surface is shown in red (black) and the average over all three oxygen atoms in the unit cell of the 1/3 ML hydrogen-covered surface is shown in gray. (b) O-2p states shown in detail. (c) Local DOS per atom for the oxygen atom located directly under the hydrogen atom in the 1/3 ML hydrogen-covered surface.

atom. Here the O-2*p* level is fully suppressed at the Fermi level. The DFT results suggest that the hydrogen effect is very local, and it is expected that there is not much overlap between charge densities of different oxygen atoms. The results of the 1/3 ML hydrogen-covered surface may also explain the small shift of the filled states toward the Fermi level observed on the O-polar surface.<sup>5</sup> A surface with such electronic states would not truly behave metallic since the flow of electrons would be impeded by the disordered hydrogen on the surface.

## VI. CONCLUSIONS

Understanding oxide surfaces, even simple ones, can be very challenging. Through the combination of low-current DLD-LEED and DFT calculations, we have been able to

investigate the surface structure of the O-polar ZnO (1×1) surface. As the (1×1) surface is not reconstructed in an ordered fashion, other mechanisms for stabilization have been considered. Our structural results are not in agreement with previous studies that suggest a clean surface with metallization as the stabilizing force. Instead, our results support a fractional monolayer of disordered hydrogen adsorbed to oxygen sites. Since a stable surface seems to exist with such a small quantity of hydrogen, we suggest that further studies be conducted in low H environments to fully explore the impact of hydrogen.

## ACKNOWLEDGMENT

This work was supported in part by DOE Grant No. DE-FG02-84ER45076.

\*cjhirsch@uwm.edu

<sup>1</sup>Ü. Özgür, Ya. I. Alivov, C. Liu, A. Teke, M. A. Reschchikov, S. Doğan, V. Avrutin, S. J. Cho, and H. Morkoç, *J. Appl. Phys.* **98**, 41301 (2005).

<sup>2</sup>A. Kobayashi, Y. Kawaguchi, J. Ohta, H. Fujioka, K. Fujiwara, and A. Ishii, *Appl. Phys. Lett.* **88**, 181907 (2006).

<sup>3</sup>P. W. Tasker, *J. Phys. C* **12**, 4977 (1979).

<sup>4</sup>C. Noguera, *J. Phys.: Condens. Matter* **12**, R367 (2000).

<sup>5</sup>O. Dulub, L. A. Boatner, and U. Diebold, *Surf. Sci.* **519**, 201 (2002).

<sup>6</sup>O. Dulub, U. Diebold, and G. Kresse, *Phys. Rev. Lett.* **90**, 016102 (2003).

<sup>7</sup>S. H. Overbury, P. V. Radulovic, S. Thevuthasan, G. S. Herman, M. A. Henderson, and C. H. F. Peden, *Surf. Sci.* **410**, 106 (1998).

<sup>8</sup>N. Jedrecy, S. Gallini, M. Sauvage-Simkin, and R. Pinchaux, *Phys. Rev. B* **64**, 085424 (2001).

<sup>9</sup>A. Wander, F. Schedin, P. Steadman, A. Norris, R. McGrath, T. S. Turner, G. Thornton, and N. M. Harrison, *Phys. Rev. Lett.* **86**, 3811 (2001).

<sup>10</sup>M. Kunat, S. G. Girol, Th. Becker, U. Burghaus, and Ch. Wöll, *Phys. Rev. B* **66**, 081402(R) (2002).

<sup>11</sup>S. T. King, S. S. Parihar, K. Pradhan, H. T. Johnson-Steigleman, and P. F. Lyman, *Surf. Sci.* **602**, L131 (2008)

<sup>12</sup>B. Meyer, *Phys. Rev. B* **69**, 045416 (2004).

<sup>13</sup>D. Human, X. F. Hu, and C. J. Hirschmugl, *Rev. Sci. Instrum.* **77**, 1 (2006).

<sup>14</sup>S. E. Chamberlin, H. C. Poon, D. K. Saldin, and C. J. Hirschmugl, *Surf. Sci.* **603**, 3367 (2009).

<sup>15</sup>A. Barbieri and M. A. Van Hove, Symmetrized Automated Tensor LEED package, available from M. A. Van Hove.

<sup>16</sup>For program description, see [<http://www.flapw.de>].

<sup>17</sup>J. B. Pendry, *J. Phys. C* **13**, 937 (1980).

<sup>18</sup>P. E. Blöchl, *Phys. Rev. B* **50**, 17953 (1994).

<sup>19</sup>G. Kresse and D. Joubert, *Phys. Rev. B* **59**, 1758 (1999).

<sup>20</sup>G. Kresse and J. Hafner, *Phys. Rev. B* **47**, R558 (1993).

<sup>21</sup>G. Kresse and J. Hafner, *J. Phys.: Condens. Matter* **6**, 8245 (1994).

<sup>22</sup>G. Kresse and J. Furthmüller, *Phys. Rev. B* **54**, 11169 (1996).

<sup>23</sup>G. Kresse and J. Furthmüller, *Comput. Mater. Sci.* **6**, 15 (1996).

<sup>24</sup>J. P. Perdew, K. Burke, and M. Ernzerhof, *Phys. Rev. Lett.* **77**, 3865 (1996); **78**, 1396 (1997).

<sup>25</sup>V. E. Henrich, H. J. Zeiger, E. I. Solomon, and R. R. Gay, *Surf. Sci.* **74**, 682 (1978).

<sup>26</sup>B. Meyer and D. Marx, *Phys. Rev. B* **67**, 035403 (2003).

<sup>27</sup>C. B. Duke and A. R. Lubinsky, *Surf. Sci.* **50**, 605 (1975).

<sup>28</sup>W. Göpel, J. Pollmann, I. Ivanov, and B. Reihl, *Phys. Rev. B* **26**, 3144 (1982).

<sup>29</sup>V. K. Lazarov, R. A. Plass, H. C. Poon, D. K. Saldin, M. Weinert, S. A. Chambers, and M. Gajdardziska-Josifovska, *Phys. Rev. B* **71**, 115434 (2005).